Liquid Crystals
Publication details, including instructions for authors and subscription information:
http://www.informaworld.com/smpp/title~content=t713926090

Oligomeric 1,3,5-triazines containing disc-shaped penta-alkyne and triphenylene side groups

D. Janietz[a]; R. Festag[b]; C. Schmidt[b]; J. H. Wendorff[b]
[a] Research Group Thin Organic Layers, Potsdam University, tow, Germany [b] Institute of Physical Chemistry and Centre of Material Science, Philipps-University, Marburg, Germany

To cite this Article Janietz, D. , Festag, R. , Schmidt, C. and Wendorff, J. H.(1996) 'Oligomeric 1,3,5-triazines containing disc-shaped penta-alkyne and triphenylene side groups', Liquid Crystals, 20: 4, 459 — 467
To link to this Article: DOI: 10.1080/02678299608032060
URL: http://dx.doi.org/10.1080/02678299608032060

LIQUID CRYSTALS, 1996, VOL. 20, NO. 4, 459-467

Oligomeric 1,3,5-triazines containing disc-shaped penta-alkyne and triphenylene side groups

by D. JANIETZ*
Research Group Thin Organic Layers, Potsdam University, Kantstr. 55,
D-14513 Teltow, Germany

R. FESTAG, C. SCHMIDT and J. H. WENDORFF
Institute of Physical Chemistry and Centre of Material Science,
Philipps-University, Hans-Meerwein-Str., D-35032 Marburg, Germany

(*Received 21 June 1995; in final form 9 November 1995; accepted 28 November 1995*)

A new type of discotic oligomer systems has been realized with either penta-alkyne or triphenylene side groups attached to amino substituted 1,3,5-triazine units in the main chain. The synthesis was carried out by reaction of 2,4-dichloro-1,3,5-triazine modified penta-alkynes and triphenylenes, respectively, with hexamethylene diamine. The discotic oligomers form stable edge-on oriented monolayers at the air/water interface. The mesophase structure of the novel discotic oligomers is characterized by an unusual lamellar layer arrangement. The mesogenic layer structure of the oligomeric triphenylenes changes to a rectangular columnar arrangement by charge transfer interaction with 2,4,7-trinitrofluorenone (TNF). Dielectric investigations were performed on the oligomeric triphenylene systems to analyse the influence of flexible segments on the internal mobility within the condensed state.

1. Introduction

The mesomorphic properties of discotic liquid crystals, first studied in 1977 [1], result predominantly from the form-anisotropic shape of the rigid central molecular part. The type of thermally induced discotic mesophase depends mainly on the chemical nature of the disc-shaped cores. Thus, triphenylenes substituted with long aliphatic chains usually exhibit discotic hexagonal ordered (D_{ho}) mesomorphic structures [2] characterized by a columnar organization of the single molecules and a hexagonal arrangement of the columns. In contrast, disc-shaped multi-alkynylbenzene derivatives form the rarely observed nematic discotic (N_D) phase [3, 4].

On the other hand, organic compounds containing electron donor units can be doped with acceptor molecules and both electron-rich systems, triphenylenes as well as multi-alkynes, are known to form charge-transfer complexes with rather flat but non-liquid crystalline electron acceptors like 2,4,7-trinitrofluorenone (TNF) [5]. Donor-acceptor interaction may lead to variations as well as to the induction of hexagonal columnar ordered mesophases [5-8]. Furthermore, binary systems of disc-like donor and acceptor molecules have been described which exhibit the so-called nematic columnar (N_C) phase [8-11].

Discotic systems, i.e. discotic amphiphiles, have also been investigated with respect to molecular arrangements at the air/water interface. The types of molecular organization within these monolayers are quite different from those of classical amphiphiles and depend on the chemical nature of the disc-shaped cores. Strong core-water interaction leads to a side-on orientation as observed for azamacrocycles [12, 13], whereas it was found that asymmetric discotic penta-alkynes, as well as triphenylenes substituted by terminal polar head groups [8, 14], form edge-on oriented monolayers at the water surface [14-17]. Highly organized molecular structures were realized on solid substrates by the Langmuir-Blodgett (LB) technique [15-19].

A further approach towards controlling supramolecular columnar structures at interfaces, as well as in the mesomorphic bulk state, involves the attachment of discotic groups to a polymer backbone. Discotic polymers combine two characteristic features, the tendency of the disc-shaped moieties to self-organize and the tendency of flexible main chain or spacer segments to destroy such a structure formation. Compared with calamitic polymers, the variety of discotic polymers described in the literature is still rather limited [20]. Discotic triphenylene side chain polymers investigated so far are characterized by the attachment of triphenylene groups to polysiloxane [21, 22], polyacrylate [6, 22], polymethacrylate [6, 22] and

---

*Author for correspondence.

0267-8292/96 $12·00 © 1996 Taylor & Francis Ltd.

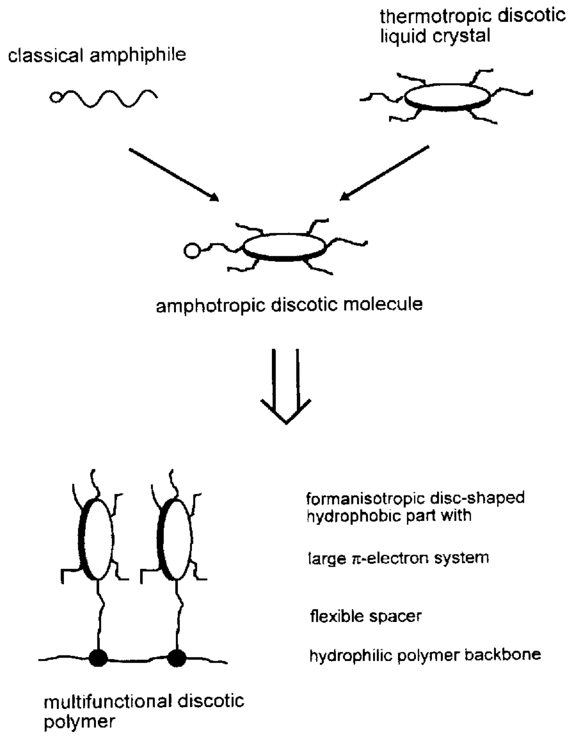

Figure 1. Generation of functional discotic polymers.

polyester [6] backbones. Depending on the chemical nature of the main chain and/or the spacer length, these polymers were found to be amorphous [6, 22] or to form columnar mesomorphic structures with either hexagonal or rectangular lattices [22].

We present a novel type of oligomeric discotics which are characterized by the attachment of either triphenylene or penta-alkyne side groups to amino substituted 1,3,5-triazine moieties in the main chain. The concept consists in introducing a functional hydrophilic backbone having the tendency to self-organize via hydrogen bonding (figure 1). We will focus on the synthesis, the behaviour at the air/water interface, the thermal properties and the mesomorphic behaviour of binary systems obtained by doping with TNF.

2. Results and discussion

2.1. *Synthesis*

The synthesis of the new triazine oligomers **5** and **6** containing disc-shaped side groups was carried out starting from cyanuric chloride. Treatment with either the hydroxy substituted penta-alkynylbenzene ethers **1a, b** [8, 17] or alkoxytriphenylenes **2a, b** containing just one hydroxy function [14, 22, 24], respectively, resulted in the disc-shaped intermediates **3** and **4** modified by a reactive difunctional dichloro-1,3,5-triazine substituent. Applying reaction conditions according to an improved method for the synthesis 2-alkoxy-4,6-dichloro-1,3,5-triazines [23], the yields of compounds **3** and **4** were 70 to 80 per cent after purification. Subsequent phase transfer catalysed reaction of **3** and **4** with hexamethylene diamine yielded the discotic oligomers **5** and **6**. GPC analyses of the discotic triazine oligomers **5** and **6** revealed co-existence of up to pentameric structures ($n = 3$ to 5).

The only by-products isolated from the reaction sequence presented in figure 2 resulted from exchange of the hydroxy substituents of **1** and **2** for chlorine, leading simply to the appropriate discotic alkyl chlorides.

Several modifications were performed to study the influence of the chemical primary structures of the new discotic oligomers on supramolecular structure formation. By keeping molecular parameters of the novel main chain type constant, different kinds of discotic side groups were attached. Whereas the oligomeric penta-alkynes **5** are characterized by different lateral substituents (pentyl or hydrogen), the five-fold pentyloxy substituted triphenylene side groups of the triazine oligomers **6** are decoupled from the main chain by alkyl spacers of different length.

2.2. *Monolayers of the oligomeric discotic triazines* **5** *and* **6** *at the air/water interface*

Both disc-shaped groups of asymmetric low molar mass triphenylenes, as well as penta-alkynes are known to be hydrophobic [14, 17]. By attaching the hydrophobic discotic groups to the polar diamino substituted 1,3,5-triazine moieties we expected that amphiphilic properties may be induced. Indeed, all oligomers **5** and **6** form stable monolayers when spread from their chloroform solutions on the water surface. The surface (π) – area (A) isotherms show no phase transitions during compression, but a direct transition to a solid condensed form. Collapse areas of the penta-alkynes **5a** and **5b** are 0·8 and 0·6 nm^2/side group, respectively, clearly indicating the additional area requirement of the five lateral pentyl chains of the pentayne side groups of **5a**.

Surprisingly, collapse areas of the oligomeric triphenylenes **6a, b** show similar differences (**6a**: 0·75 nm^2; **6b**: 0·55 nm^2) although the substitution pattern at the lateral sphere of the triphenylene groups is the same for both oligomers **6a** and **6b**.

The observed values indicate an edge-on arrangement with a molecular orientation of the hydrophobic discotic side groups perpendicular to the water surface for each triazine oligomer **5** and **6**.

To obtain further information on the monolayer behaviour of the discotic oligomers **5** and **6**, a comparison with the appropriate amphiphilic hydroxy substituted monomers **1** and **2** is essential. An increased mono-film stability is found for the oligomeric triazines **5a, b** and **6b** (figure 3) which has to be assigned to the special type of

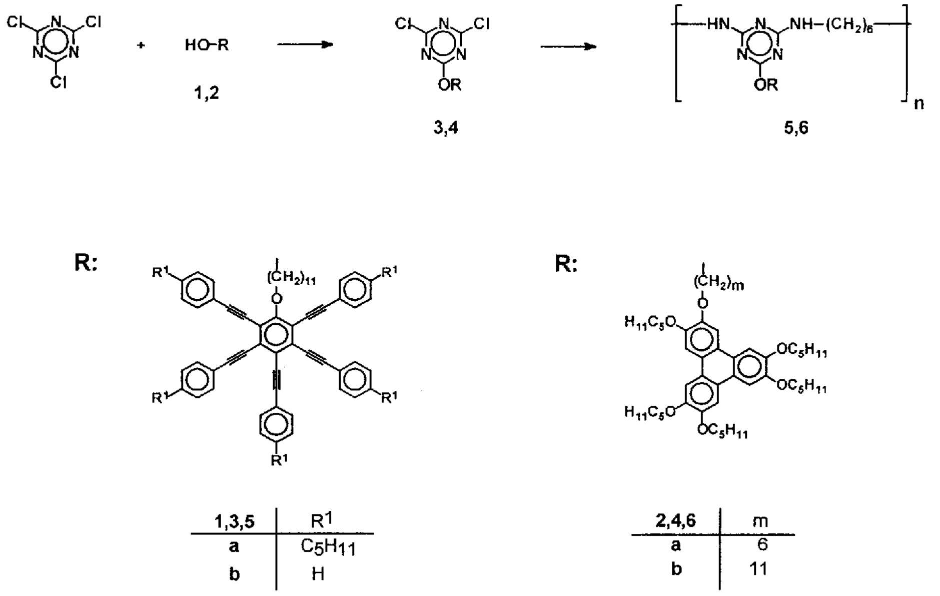

Figure 2. Synthetic route to the 1,3,5-triazine modified oligomers **5** and **6** containing disc-shaped penta-alkyne and triphenylene side groups.

hydrophilic amino triazine modified backbone with an enlarged affinity for the water surface compared that for the hydroxy head groups of **1** and **2**. But there is no significant difference between the collapse areas of **5a, b** and **6b** compared to the appropriate monomeric penta-alkynes **1a, b** and the amphiphilic triphenylene **2b**, indicating that the main chain does not require additional area within the compressed monolayers. The only exception is the oligomeric triphenylene **6a**, containing a six methylene group spacer, which shows a slight decrease of collapse pressure compared to the corresponding triphenylenyloxy-hexanol **2a** (the monolayer behaviour of **2a** has already been described in [14]) and an increased collapse area as mentioned above.

The monolayer assembly of the discotic amphiphiles **5** and **6**, as concluded from the experimental data, is presented schematically in figure 4. Only the amino substituted 1,3,5-triazine moieties serve as anchor groups for the edge-on oriented penta-alkyne or triphenylene hydrophobic side groups, while the connecting methylene groups of the main chains form conformations away from the water surface.

The described abnormal behaviour of the triphenylene **6a** is considered to confirm the structure model given in figure 4. Considering an almost stretched conformation of the spacer methylene groups, there is no influence of the spacer chain length on the occupied area/molecule within the compressed monolayers. But the available space between the water and the edge-on arranged triphenylene cores of **6a, b** is limited by the length of the all-*trans* arranged spacers. An optimum filling of this space with closely packed hydrophobic main chain methylene groups is possible in the case of triphenylene oligomer **6b**, characterized by spacer sequences with 11 methylene groups. In contrast, a decrease of the spacer length may lead to the consequence that parts of the hydrophobic alkyl chains connecting the triazine groups of the main chains retain contact with the water surface, thus leading to less stable monolayers and an increase of the collapse area as observed for **6a**.

The non-occurrence of such a destabilizing effect in the case of the pentayne oligomers **5** can be explained by the longer spacer groups compared to **6a**. Molecular mechanics simulations of molecular packing of LB multilayers derived from monomeric amphiphilic penta-alkynes in fact showed several possibilities for an interdigitated packing of flexible segments independent of the lateral substitution patterns [17].

2.3. *Thermal behaviour of the triazine modified discotic penta-alkynes and triphenylenes*

The disc-shaped intermediates **3** and **4** do not exhibit mesomorphism. Obviously, the introduction of the bulky dichloro-1,3,5-triazine substituent in the lateral sphere of the multi-alkyne, as well as the triphenylene cores, causes a considerable degree of disturbance of the form-anisotropy resulting in a suppression of mesogenic structure formation of the pure compounds. Enantiotropic mesophases are induced by charge transfer interactions of **3** and **4** with 2,4,7-trinitrofluorenone (TNF). The phase transition data for the binary systems (equimolar mixtures) obtained by such doping are summarized in table 1.

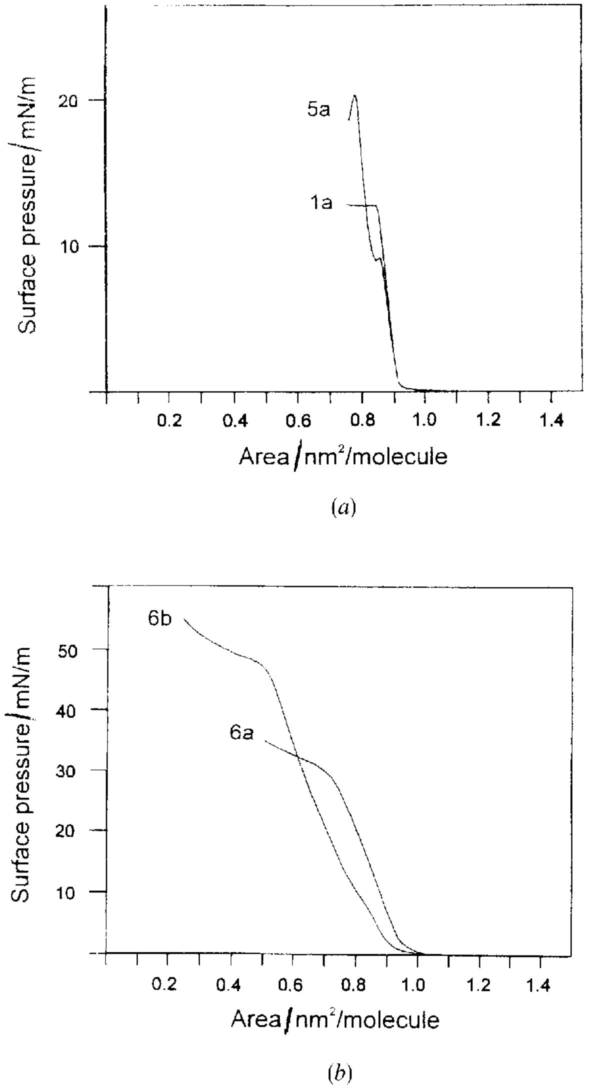

Figure 3. Surface pressure-area isotherms: (*a*) π/A-isotherms of the amphiphilic penta-alkyne oligomer **5a** and of the corresponding hydroxy substituted monomeric pentayne **1a**: (*b*) π/A-isotherms of the discotic triphenylene oligomers **6a, b**.

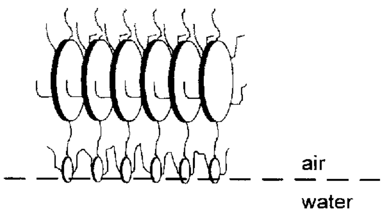

Figure 4. Schematic presentation of the edge-on orientation of the amphiphilic discotic oligomers **5** and **6** at the air/water interface.

Optical microscopy of the donor acceptor complexes derived from mixing the pentaynes **3** with TNF shows schlieren textures typical of nematic mesophases. The transition enthalpies to the isotropic state (table 1) are of the same order of magnitude as observed for pure discotic multi-alkynes forming nematic discotic (N_D) mesophases [3, 4] and indicate the occurence of N_D phases in binary systems derived from **3a** and **3b**, also. This behaviour is quite different from that observed for the hydroxy modified penta-alkynes **1a, b**, which exhibit either CT-induced discotic hexagonal ordered (**1a**) or nematic columnar (**1b**) mesophases depending on the lateral substitution pattern [8, 17]. These differences clearly demonstrate that the disturbing effect of the dichloro-triazine substituent also influences the structure formation induced by EDA-interactions. In contrast, the CT complexes obtained from the laterally triazine substituted triphenylenes **4** form columnar mesophases easily identified by their typical textures.

The thermal behaviour of the triazine modified triphenylene oligomers **6a, b** is characterized by a glass transition (for further details see §2.5.), followed by an endotherm indicating the transition to the isotopic state. The pentyl substituted oligometric penta-alkyne **5a** shows a clearing transition temperature at 158°C, but no T_g until room temperature, whereas for the laterally unsubstituted pentayne **5b**, only a glass transition is detectable by DSC (table 2).

Doping of the triphenylene oligomers **6a, b** with TNF results in an increase of the clearing temperatures of the binary systems compared to the pure triphenylenes. This behaviour reveals the existence of mesophases at least for the oligomers **5a** and **6a, b**, as well as for CT-complexes obtained from the triphenylenes **6**.

Optical microscopy, however, shows only untypical textures for the pure discotic oligomers and for the EDA-complexes. Consequently, X-ray investigations were performed to identify the types of mesophase structures of the novel discotic oligomers.

2.4. *X-ray investigations*

The X-ray diagrams characteristic of the mesophases of the oligomers display in all cases a set of narrow reflections in the small angle region and a halo at larger scattering angles. Figure 5 displays as an example the diagram obtained for compound **6b**. It is obvious that a layer structure exists; no mixed reflections were found. The layer structure is characterized by very small longitudinal displacement, since layer reflections up to the 9th order were detected. The occurence of the halo arises from the presence of only a short range order within the layers. The structure displayed by the oligomers with disc-like groups corresponds therefore to a smectic A

Table 1. Phase transition data (°C) for the charge transfer complexes of the monomeric dichlorotriazines **3** and **4** with 2,4,7-trinitrofluorenone (equimolar mixtures) determined by differential scanning calorimetry (10 K min^{-1}); transition enthalpies (kJ mol^{-1}) are given in brackets.

Compound	Cr		D_{ho}		N_D		I
3a	–		–		●	54·1 (0·39)	●
3b	●	74·7 (7·27)	–		●	102·0 (0·26)	●
4a	–		●	143·7 (0·83)	–		●
4b	–		●	65·3 (0·40)	–		●

Cr = Crystalline; D_{ho} = hexagonal columnar ordered; N_D = nematic discotic; I = isotropic.

type arrangement, which is highly surprising. The magnitude of the layer dimensions which amounts, for instance, to 48·8 Å in the case of compound **6b** and 43·3 Å in the case of compound **6a** indicates that a single layer arrangement is not involved, but rather a double layer arrangement. Figure 6 illustrates such a structure in the case of the triphenylene systems.

Such a double layer structure is stabilized by the formation of hydrogen bonds between the polymer backbone segments. The presence of hydrogen bonds was checked by IR spectroscopic investigations. The IR spectra of the thermally untreated triazine oligomers **5** and **6** (KBr pellets) show several absorptions in the region of the NH-stretching vibrations above 3100 cm^{-1}. Thin films of the oligomer **6a** were prepared on a germanium substrate for IR investigations of thermally treated samples. After annealing at certain temperatures within the mesophase range, the IR spectra show the appearance of an additional peak at 3470 cm^{-1}. This peak is no longer present after heating the samples to the isotropic state. We attribute the temperature dependent spectroscopic behaviour to intermolecular interactions between the amino substituted triazine main chains promoted by hydrogen bonding present only within the mesophase. Similar behaviour has been discussed for mesomorphic compounds based on two 1,3,5-triazine units connected by a flexible alkylamino spacer [25]. It is thus apparent that the interactions between the backbone segments frustrate the structure preferred by the disc-like units.

Table 2. Glass temperatures and clearing temperatures (°C) of the discotic oligomers **5** and **6** and of the corresponding charge transfer complexes.

Sample	**5a**	**5b**	**6a**	**6b**	**6b**/TNF (1:1)	**6a**/TNF (1:1)	**6a**/TNF (2:1)
T_g	–	112	41	71	47	–	–
T_i	158	–	121	136	154	182	195

T_g = glass temperature; T_i = clearing temperature.

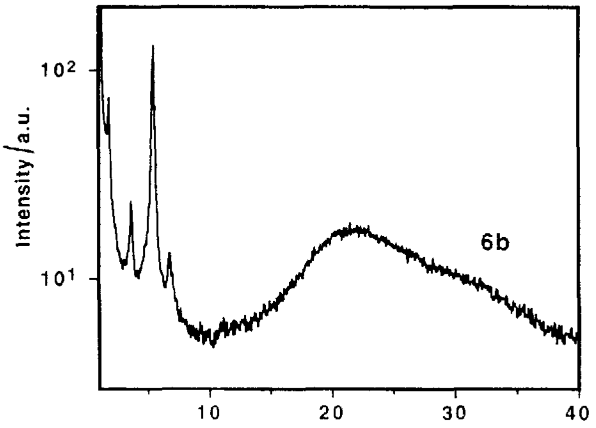

Figure 5. WAXS-diagram of compound **6b** (T = 90°C).

The test this structural model we performed computer simulations by means of the force field DREIDING II [26] for the compounds **5a**, **6a** and **6b**, and compared the predicted layer spacings with the observed values (see table 4). Table 4 shows that experimental and simulated values agree well. The simulations also show that the discotic mesgenic units are tilted by about 90° relative to the plane defined by the triazine backbone for steric reasons.

No mesophase was observed for the penta-alkyne oligomer **5b**; this compound crystallizes at lower temperatures. It seems that the presence of strong hydrogen bonds between the backbone units is not sufficient for the formation of a layer structure; strongly form-anisotropic units have to be present.

The experimental results on the structure of compound **6a** doped with TNF are shown in figure 7. It is apparent that the X-ray diagram is strongly modified by the dopant. The structure can be assigned to a columnar rectangular arrangement both for the case of a 1:2 and a 1:1 mixture of TNF and the compound **6a** (see table 5). No such strong effect was found for the doped compound **6b**, characterized by the longer spacer length. The mesogenic organization of mixtures from **6b** and TNF remains a lameller layer structure (layer spacing 46·95 Å).

Thus, the mesophase arrangement of the donor acceptor complexes is a function of the spacer connecting the triphenylene side groups with the main chain. These

Table 3. Bragg spacing compounds **6a**, **6b** and **5a** (in Å).

Sample	d_{100}	d_{200}	d_{300}	d_{400}	d_{500}	d_{600}	d_{700}	d_{800}	d_{900}
5a	29·14	14·72	9·79	7·36	5·89	4·89	4·22	3·28	
6b	48·59	24·16	15·28	12·80	–	–		–	–
6a	43·68	21·73	14·47	–	8·68	–	6·20	5·43	4·85

results indicate that the structures displayed by the compounds discussed here are the result of a delicate balance of interactions which compete with each other.

2.5. *Dielectric investigations*

The dielectric analysis was performed on the two triphenylene systems **6a** and **6b** to test whether the stepwise variations of the specific heat obtained in the DSC measurements actually correspond to glass transitions. A second aim was to analyse the influence of the spacer length on the internal mobility within the condensed state. The dielectric analysis revealed in both cases the presence of three distinct relaxation processes as shown in figure 8. The two low temperature relaxations (γ and β) display a low relaxation strength and a similar activation energy. They can both be attributed to secondary relaxations and show an Arrhenius type temperature/frequency relation (figure 9 and Table 6).

No significant influence of the spacer length on the internal mobility was detected. We have to assume a motion of the alkoxy side chains in the lateral sphere of the mesogens. Based on the values found for the activation energies and the characteristic temperatures of the relaxation processes, we assign these processes tentatively to a rotational and a tilting motion of the alkoxy side chains of the mesogens [27].

The high temperature relaxation displays a WLF-behaviour as apparent from the activation diagram shown in figure 10 [28]. It can thus be attributed to a glass relaxation. The glass transition temperatures, as extrapolated to low frequencies (0·01 Hz), coincide in both cases with those found by the calorimetric studies

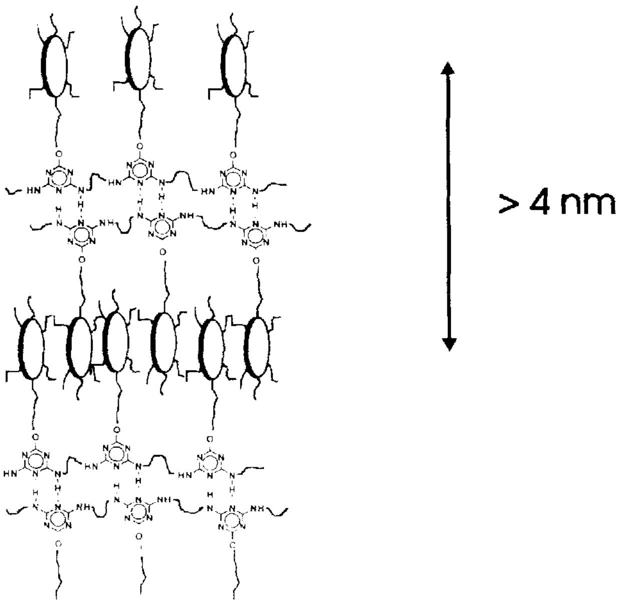

Figure 6. Model for the S_A-like phase of the triphenylene systems **6**.

Table 4. Computer simulation of the layer spacings of the structures and experimental values in comparison.

Sample	*a* (exp) / Å	*a* (sim) / Å
6b	48·81	49·66
6a	43·34	41·61
5a	29·43	29·55

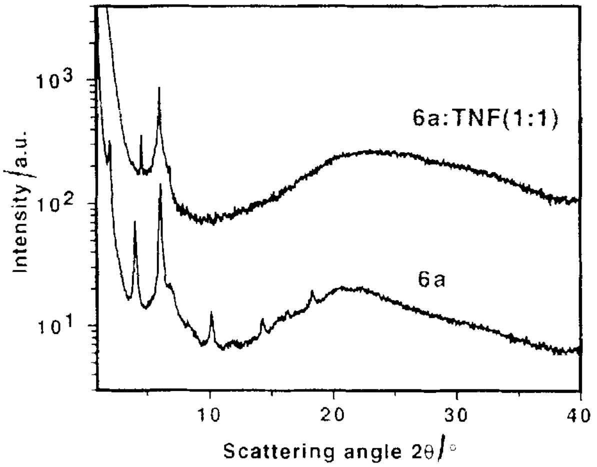

Figure 7. WAXS-diagram of compound **6a** ($T = 115°C$) and **6a**/TNF(1 : 1)($T = 83°C$).

Table 5. Layer spacings of CT-complexes **6a**/TNF(1 : 1) and **6a**/TNF(2 : 1).

Sample	d_{100}	d_{200}	d_{110}	d_{300}	*a*/Å	*b*/Å
6a/TNF(2 : 1)	41·06	20·84	16·32	13·96	41·52	16·82
6a/TNF(1 : 1)	39·04	19·42	14·67	12·94	38·91	15·83

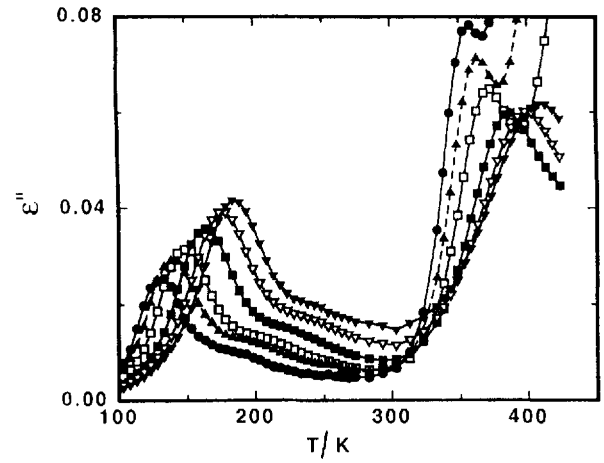

Figure 8. Dielectric data for compound **6a** at different frequencies. ● 2·68*102 Hz; ▲ 1*103 Hz; □ 3·75*103 Hz; ■ 2·67*104 Hz; ▽ 1*105 Hz; ▼ 2·5*105 Hz.

(see table 6). The values of the WLF parameters are also typical for polymeric systems [28]. It is thus possible to freeze in the unusual new lameller mesophase structure of the triazine based discotic side group polymers at temperatures well above room temperature.

3. Conclusions

The novel architecture of the triazine based backbone leading to the formation of hydrogen bonds between the backbone segments give rise to a richness in phase formation. The oligomers form on the one hand stable monolayers at the air/water interface and on the other hand a lamellar S_A-like arrangement in the condensed state. A columnar structure can be induced in certain cases by doping with an acceptor. It thus seems that the concept of introducing a competition between structure forming tendencies of the backbone and of the side groups offers novel modes of controlling liquid crystalline structures.

Table 6. Activation energies for the low temperature relaxation processes and glass temperatures (Dielectric Spectroscopy and DSC) of compounds **6a** and **6b**.

Sample	Tg/°C (DSC)	Tg/°C (DK)	$E_{\mathrm{akt}}\gamma$/ kJmol^{-1}	$E_{\mathrm{akt}}\beta$/ kJmol^{-1}	ε(γ,β)	ε(α)
6b	71·4	68·9	–	50·75	0·2	0·5
6a	41·5	46·7	26·45	50·88	0·15	0·2

4. Experimental

4.1. *Synthesis of compounds*

The synthesis of the hydroxyalkyl pentakis(phenylethynyl)phenyl ethers **1a, b** used for the preparation of the penta-alkynyl substituted dichloro-triazines **3a, b** has been described previously [8, 17]. The desired 2-(ω-hydroxyalkyloxy)-3,6,7,10,11-pentakis(pentyloxy) triphenylenes **2a, b** [24] were obtained by deacetylating etherification of 3,6,7,10,11-pentakis(pentyloxy)-2-triphenylenyl acetate (triphenylene monoacetate) [21] either with 6-chlorohexanol or 11-bromo-undecanol.

To prepare the 2,4-dichloro-1,3,5-triazine modified disc-shaped penta-alkynylbenzene derivatives **3** and the triphenylenes **4**, 184·5 mg (1 mmol) of cyanuric chloride, 1 mmol of the appropriate hydroxy substituted pentaynes **1** or of the triphenylenyloxy alkanols **2** and 261·4 mg (277·5 ml; 3 mmol) of *N*,*N*-dimethylacetamide in 40 ml of dichloromethane were stirred for 5 days at 35°C. After cooling to room temperature, the solution was diluted to a total volume of 100 ml with dichloromethane and washed with water. After drying the

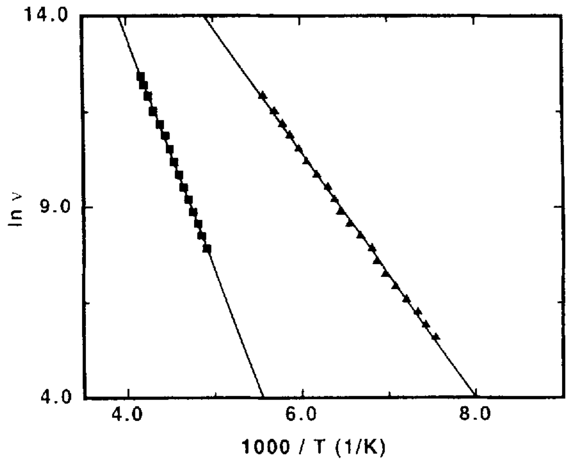

Figure 9. Arrhenius diagram (and relaxation) of compound **6a**. ▼ $E_{akt}(\gamma)=26{\cdot}45$ kJ mol^{-1}; ■ $E_{akt}(\beta)=50{\cdot}88$ kJ mol^{-1}.

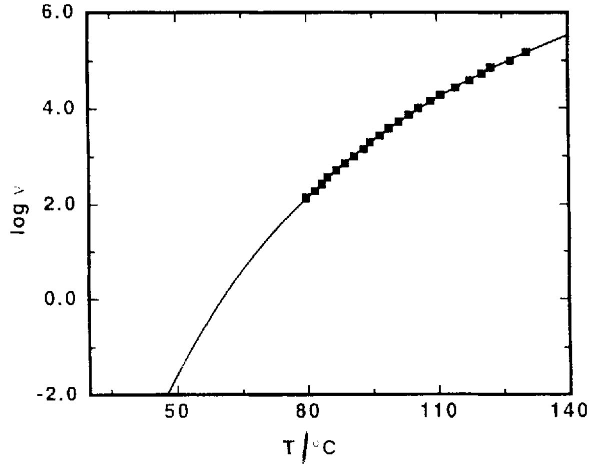

Figure 10. WLF-diagram of compound **6a** (*T*g=47·65°C; $C_1=13{\cdot}37$; $C_2=71{\cdot}67$°).

organic solution with magnesium sulphate and evaporation of the solvent, the crude products **3** and **4** were purified by flash chromatography using Kieselgel 60, 230–400 mesh (E. Merck, Darmstadt, Germany).

2,4-Dichloro-6-{11-[pentakis((4-pentylphenyl)ethynyl) phenoxy]undecyl-1-oxy}-1,3,5-triazine **3a.** Yield 71·3 per cent. Mp 66°C (eluent for chromatographic purification: light petroleum/ethyl acetate 20:1). $C_{85}H_{97}Cl_2N_3O_2$ (1263·7). IR (KBr): $\nu = 2206$, 1541, 1501, 1485, 1374, 1349, 1249 cm^{-1}. ^{1}H NMR ($CDCl_3$): δ (ppm) = 7·60–7·48 (m; 10H, phenyl-H), 7·25–7·10 (m; 10H, phenyl–H), 4·49 (t, $J = 6{\cdot}5$ Hz; 2H, CH_2–O–triazine), 4·38 (t, J = 6·5 Hz; 2H, CH_2–O–phenyl), 2·61 (t, J = 7·5 Hz; 10H, phenyl CH_2), 1·92 (m; 2H, CH_2, undecyl chain), 1·79 (m; 2H, CH_2 undecyl chain), 1·73–1·51 (m; 2H and 10H, CH_2, undecyl and pentyl chains, respectively), 1·48–1·20 (m; 12H and 20H, CH_2, undecyl and pentyl chains, respectively), 0·91 (t, $J = 7$ Hz; 15H, CH_3). MS(FD): $m/e = 1264$ ($M^+ + 3$).

2,4-Dichloro-6-{11-[pentakis(phenylethynyl)phenoxy] undecyl-1-oxy}-1,3,5-triazine **3b**. Yield 69·4 per cent. Mp 135°C (eluent for chromatographic purification: chloroform). $C_{60}H_{47}Cl_2N_3O_2$ (913·0). IR (KBr): $\nu = 2206$, 1544, 1504, 1369, 1355, 1252 cm^{-1}. ^{1}H NMR ($CDCl_3$): δ (ppm) = 7·70–7·53 (m; 10H, phenyl–H), 7·45–7·30 (m; 15H, phenyl-H), 4·47 (t, $J = 6{\cdot}5$ Hz; 2H, CH_2–O–triazine), 4·40 (t, $J = 6{\cdot}5$ Hz; CH_2–O–phenyl), 1·92 (m; 2H, CH_2), 1·79 (m; 2H, CH_2), 1·60 (m; 2H, CH_2), 1·50–1·15 (m; 12H, CH_2). MS (FD): $m/e = 912$ ($M^+ + 1$).

2,4-Dichloro-6-{6-[3,6,7,10,11-pentakis(pentyloxy)-2-triphenylenyloxy]hexyl-1-oxy}-1,3,5-triazine **4a**. Yield 74·1 per cent. Mp 72°C (eluent for chromatographic purification: chloroform). $C_{52}H_{73}Cl_2N_3O_7$ (923·1). IR (KBr): $\nu = 1544$, 1516, 1446, 1388, 1370, 1261 cm^{-1}. ^{1}H NMR ($CDCl_3$): δ (ppm) = 7·83 (s; 6H, phenyl–H), 4·50 (t, $J = 6{\cdot}5$ Hz; 2H, CH_2–O–triazine), 4·21 (t, $J = 6{\cdot}5$ Hz; 12H, CH_2–O–phenyl), 1·94 (m; 12H, CH_2), 1·78–1·37 (m; 26H, CH_2), 0·97 (t, $J = 7$ Hz; 15H, CH_3). MS (FD): $m/e = 921$ (M^+).

2,4-Dichloro-6-{11-[3,6,7,10,11-pentakis(pentyloxy)-2-triphenylenyloxy]undecyl-1-oxy}-1,3,5-triazine **4b**. Yield 79·3 per cent. Oil (eluent for chromatographic purification: 1. chloroform; 2. chloroform/methanol 100:1). $C_{57}H_{83}Cl_2N_3O_7$ (993·2). ^{1}H NMR $CDCl_3$): δ (ppm) = 7·81 (s; 6H, phenyl-H), 4·43 (t, $J = 6{\cdot}5$ Hz; 2H, CH_2–O triazine), 4·21 (t, J = 6·5 Hz; 12H, CH_2–O phenyl), 1·93 (m; 12H, CH_2), 1·77 (m; 2H, CH_2), 1·58–1·23 (m; 34H, CH_2), 0·95 (t, J = 7 Hz; 15H, CH_3).

The synthesis of the oligomeric, discotic side groups containing 1,3,5-triazines **5** and **6** was carried out according to the following procedure. 0·443 mmol of the appropriate dichloro-triazine **3** and **4** was dissolved in 4 ml of nitrobenzene. After the solution cleared a mixture of 55·43 mg (0·477 mmol) of 1,6-diaminohexane, 83·7 mg (1 mmol) of sodium bicarbonate, 20·0 mg (0·048 mmol) of benzyldimethylhexadecyl ammonium chloride, 2 ml of water and 0·2 ml of dioxane was added. The reaction mixture was stirred vigorously for 4 days at 85°C. The solution was cooled to room temperature and 200 ml of methanol was added. The resulting precipitates were collected by filtration and washed carefully with methanol. Purification was performed by dissolving the products in chloroform and reprecipitating with methanol. After this procedure the oligomers **5** and **6** were dried in a vacuum. Phase transition data for the compounds **5** and **6**, as well as for the charge transfer complexes derived therefrom, are collected in table 2.

Oligo[6-{11-[pentakis((4-pentylphenyl)ethynyl) phenoxy]undecyl-1-oxy}-2,4-hexamethylenediamino-1,3,5-triazine] (**5a**, $[C_{91}H_{111}N_5O_2]_n$, MW $[1306{\cdot}93]_n$): yield 85·6 per cent.

Oligo[6-{11-[pentakis(phenylethynyl)phenoxy]undecyl-1-oxy}-2,4-hexamethylenediamino-1,3,5-triazine] (**5b**, $[C_{66}H_{61}N_5O_2]_n$, MW $[956{\cdot}25]_n$): yield 73·2 per cent.

Oligo[6-{6-[3,6,7,10,11-pentakis(pentyloxy)-2-triphenylenyloxy]hexyl-1-oxy}-2,4-hexamethylenediamino-1,3,5-triazine] (**6a**, $[C_{58}H_{87}N_5O_7]_n$, MW $[966{\cdot}37]_n$): yield 88·5 per cent.

*Oligo[6-{11-[3,6,7,10,11-pentakis(pentyloxy)-2-triphenylenyloxy]undecyl-1-oxy}-2,4-hexamethylenediamino-*1,3,5-*triazine]* (**6b**, $[C_{63}H_{97}N_5O_7]_n$, MW $[1036{\cdot}50]_n$): yield 79·5 per cent.

Structural proof for the new oligomeric triazines **5** and **6** is based on spectroscopic data which are summarized in table 7.

4.2. *Preparation of the charge transfer complexes*

The donor–acceptor complexes were obtained by mixing solutions of the penta-alkynyl or triphenylene derivatives **3–6** with 2,4,7-trinitrofluorenone as electron acceptor in dichloromethane, evaporating the solvent and drying the residues in vacuum. Molar ratios of the components and phase transition data for the CT complexes are given in tables 1 and 2.

4.3. *Instrumental*

IR spectra were recorded using an FT-IR spectrophotometer 5DXC (Nicolet). ^{1}H NMR spectra were obtained with a Bruker AC200 instrument. For mass spectra, a MAT 90 (Finnigan MAT) spectrometer was used. GPC analyses were performed on PLGel columns (Waters Liquid Chromatograph) at ambient temperature with tetrahydrofuran as eluent and polystyrene standard. Spreading experiments were carried out on pure Milli-Q water subphase at 20°C using a computer controlled film balance (Commodore PET 4032 GR) equipped with two

Table 7. Spectroscopic data for the triazine oligomers **5** and **6**.

Oligomer	IR(KBr) υ/cm^{-1}	^{1}H NMR ($CDCl_3$) δ/ppm[a]
5a	3255, 2206, 1581, 1551, 1532, 1343, 1177,	7·50 (m; 10H, phenyl), 7·18 (m; 10H, phenyl), 5·09 (m; 2H, NH), 4·35 (t, J = 6·5 Hz; 2H, CH_2-O-triazine), 4·16 (t, *J* = 6·5 Hz; 2H, CH_2-O-phenyl), 3·35 (m; 4H, CH_2-N), 2·62 (t, *J* = 7·5 Hz; 10H, phenyl-CH_2), 1·90 (m; 2H, CH_2), 1·65 (m; 14H and 4H, CH_2 side groups and main chain), 1·32 (m; 32H and 4H, CH_2 side groups and main chain), 0·90 (t, *J* = 7 Hz; 15H, CH_3)
5b	3425, 3263, 2207, 1576, 1530, 1420	7·59 (m; 10H, phenyl), 7·31 (m; 15H, phenyl), 5·13 (m; 2H, NH), 4·38 (m; 2H, CH_2-O-triazine), 4·15 (m; 2H, CH_2-O-phenyl), 3·35 (m; 4H, CH_2-N), 1·92 (m; 2H, CH_2), 1·80–1·48 (m; 4H and 4H, CH_2 side groups and main chain), 1·40–1·15 (m; 12H and 4H, CH_2 side groups and main chain)
6a	3400, 3263, 3114, 1583, 1514, 1339, 1262	7·32 (s; 6H, phenyl), 5·12 (m; 2H, NH), 4·20 (m; 14H, CH_2-O), 3·33 (m; 4H, CH_2-N), 1·96 (m; 14H, CH_2), 1·77 (m; 4H, CH_2 main chain), 1·69–1·20 (m; 24H and 4H CH_2 side groups and main chain), 0·98 (t, *J* = 7 Hz; 15H, CH_3)
6b	3263, 1583, 1517, 1467, 1436, 1262	7·84 (s; 6H, phenyl), 5·13 (m; 2H, NH), 4·25 (m; 14H, CH_2-O), 3·37 (m; 4H, CH_2-N), 1·98 (m; 14H, CH_2), 1·80–1·20 (m; 34H and 8H side groups and main chain), 0·99 (t, *J* = 7 Hz; 15H, CH_3)

[a] All signals show a greater or lesser degree of broadening compared to the corresponding monomeric dichloro-triazines **3** and **4**.

Wilhelmy pressure pick-up systems [29]. The concentrations of the spreading solutions (Chloroform, E. Merck p.a.) were approximately 0·5 mg ml^{-1}. A compression time of 20 min was used in all experiments. Texture observations were made using a Leitz Orthoplan polarizing microscope equipped with a Mettler FP 82 hot stage and an Olympus BHS polarizing microscope in conjunction with a Linkam TMS 600/S hot stage and Linkam TP 92 control unit, respectively. Microphotographs were obtained with an Olympus OM-4Ti system camera. Calorimetric investigations were performed with a Perkin-Elmer DSC-2c and a Perkin-Elmer DSC 7. Wide angle X-ray scattering analysis was performed employing a goniometer from Siemens (D 5000). Dielectric measurements were made using a Hewlett Packard Impedance Analyzer 4284 A and covered the frequency range from 10 to 10^6 Hz. The experimental set-up is described elsewhere [30].

References

[1] Chandrasekhar, S. Sadashiva, B. K., and Suresh, K. A., 1977, *Pramana*, **9,** 471.

[2] Destrade, C., Foucher, P., Gasparoux, H., Nguyen Huu Thin, Levelut, A. M., and Malthête, J., 1984, *Mol. Cryst. liq. Cryst*, **106,** 121.

[3] Kohne, B., and Praefcke, K., 1987, *Chimia*, **41,** 196.

[4] Praefcke, K., Kohne, B., and Singer, D., 1990, *Angew. Chem.*, **102,** 200.

[5] Bengs, H., Ebert, M., Karthaus, O., Kohne, B., Praefcke, K., Ringsdorf, H., Wendorff, J. H., and Wüstefeld, R., 1990, *Adv. Mater*, **2,** 141.

[6] Ringsdorf, H., Wüstefeld, R., Zerta, E., Ebert, M., and Wendorff, J. H., 1989, *Angew. Chem.*, **101,** 934.

[7] Ebert, M., Frick, G., Baehr, Ch., Wendorff, J. H., Wüstefeld, R., and Ringsdorf, H., 1991, *Liq. Cryst.*, **11,** 293.

[8] Janietz, D., Praefcke, K., and Singer, D., 1993, *Liq. Cryst.*, **13,** 247.

[9] Praefcke, K., Singer, D., Kohne, B., Ebert, M., Liebmann, A., and Wendorff, J. H., 1991, *Liq. Cryst*, **10,** 147.

[10] Praefcke, K., Singer, D., Langner, M. Kohne, B., Ebert, M., Liebmann, A., and Wendorff, J. H., 1991, *Molec. Cryst. liq. Cryst.*, **215,** 121.

[11] Bengs, H., Karthaus, O., Ringsdorf, H., Baehr, Ch., Ebert, M., and Wendorff, J. H., 1991, *Liq. Cryst.*, **10,** 161.

[12] Mertesdorf, C., and Ringsdorf, H., 1989, *Liq. Cryst.*, **5,** 1757.

[13] Mertesdorf, C., Plesnivy, T., Ringsdorf, H., and Suci, P. A., 1992, *Langmuir*, **8,** 2531.

[14] Karthaus, O., Ringsdorf, H., and Urban, C., 1991, *Makromol. Chem. Makromol. Symp.*, **46,** 347.

[15] Reiche, J., Dietel, R., Janietz, D., Lemmetyinen, H., and Brehmer, L., 1993, *Thin Solid Films*, **226,** 265.

[16] Angelova, A., Reiche, J., Ionov, R., Janietz, D., and Brehmer, L., 1994, *Thin Solid Films*, **242,** 289.

[17] Janietz, D., Hofmann, D., and Reiche, J., 1994, *Thin Solid Films*, **244,** 794.

[18] Karthaus, O., Ringsdorf, H., Tsukruk, V. V., and Wendorff, J. H., 1992, *Langmuir*, **8,** 2279.

[19] Tsukruk, V. V., Wendorff, J. H., Karthaus, O., and Ringsdorf, H., 1993, *Langmuir*, **9,** 614.

[20] Bauer, S., Plesnivy, T., Ringsdorf, H., and Schuhmacher, P., 1992, *Makromol. Chem. Makromol. Symp.*, **64,** 19.

[21] Kreuder, W., and Ringsdorf, H., 1983, *Makromol. Chem. rap. Commun.*, **4,** 807.

[22] Werth, M., and Spiess, H. W., 1993, *Makromol. Chem. rap. Commun*, **14,** 329.

[23] Janietz, D., and Bauer, M., *Synthesis*, **1993,** 33.

[24] Kreuder, W., Ringsdorf, H., Herrmann-Schönherr, O., and Wendorff, J. H., 1987, *Angew. Chem.*, **99,** 1300.

[25] Fornasier, R., Tornatore, M., and Chapoy, L. L., 1990, *Liq. Cryst.*, **8,** 787.

[26] Mayo, S. L., Olafson, B. D., and Goddard, W. A., 1990, *J. phys. Chem.*, **32,** 8897.

[27] McCrum, N. G., Read, B. E., and Williams, G. 1967, *Anelastic and Dielectric Effects in Polymeric Solids*, (London: Wiley).

[28] Williams, M. L., Landel, R. F., and Ferry, J. D., 1955, *J. am. chem. Soc.*, **77,** 3701.

[29] Albrecht, O., 1983, *Thin Solid Films*, **99,** 227.

[30] Kremer, F., Boese, D., Meier, G., and Fischer, E. W., 1989, *Progr. Colloid & Polymer Sci.*, **80,** 129.